General Disclaimer

One or more of the Following Statements may affect this Document

- This document has been reproduced from the best copy furnished by the organizational source. It is being released in the interest of making available as much information as possible.

- This document may contain data, which exceeds the sheet parameters. It was furnished in this condition by the organizational source and is the best copy available.

- This document may contain tone-on-tone or color graphs, charts and/or pictures, which have been reproduced in black and white.

- This document is paginated as submitted by the original source.

- Portions of this document are not fully legible due to the historical nature of some of the material. However, it is the best reproduction available from the original submission.

Produced by the NASA Center for Aerospace Information (CASI)

NASA Technical Memorandum 78766

RECENT DEVELOPMENTS IN ANALYSIS OF CRACK PROPAGATION AND FRACTURE OF PRACTICAL MATERIALS

(NASA-TM-78766) RECENT DEVELOPMENTS IN ANALYSIS OF CRACK PROPAGATION AND FRACTURE OF PRACTICAL MATERIALS (NASA) 20 p HC A02/MF A01 CSCL 20K

N78-30606

Unclas G3/39 28582

H. F. HARDRATH
J. C. NEWMAN, JR.
W. ELBER
C. C. POE, JR.

June 1978

National Aeronautics and Space Administration

Langley Research Center
Hampton, Virginia 23665

RECENT DEVELOPMENTS IN ANALYSIS OF CRACK PROPAGATION AND FRACTURE OF PRACTICAL MATERIALS

Herbert F. Hardrath, James C. Newman, Jr., Wolf Elber, Clarence C. Poe, Jr.
Materials Division
NASA, Langley Research Center
Hampton, Virginia 23665

INTRODUCTION

Present U.S. Air Force [1] and proposed U.S. civil [2] airworthiness regulations are based on considerations of "damage tolerance" in aircraft structures. The underlying philosophy for these regulations is to acknowledge that accidental or normal service-induced damage is inevitable and that periodic inspections are required to detect such damage. Airworthiness is then assured by demonstrating that damage that escapes one inspection will not grow to critical size before the next inspection. Two evaluations must be made: first, the rate of damage propagation under expected service loading; and second, the residual static strength in the presence of significant damage. Both of these evaluations employ fracture mechanics analyses and predictions.

Unfortunately, most fracture mechanics developments have concentrated on analysis and prediction of behavior in brittle materials and relatively simple heavy sections for which simple linear elastic analysis are adequate. In contrast, aircraft structures usually employ somewhat ductile materials, thin gages, and complex configurations. Further, complex load histories and hostile environments are generally features of most aircraft design problems. Consequently, special considerations are required to treat these problems adequately.

NASA-Langley Research Center has conducted a variety of research tasks to extend the capabilities of fracture mechanics to deal with some of these complexities. The purpose of this paper is to describe the current stage of development of these capabilities.

LIMITATIONS OF LINEAR ELASTIC FRACTURE MECHANICS

Fracture

Griffith [3] is generally cited as the earliest investigator of fracture mechanics. He was concerned with the behavior of glass, an inherently brittle material. Irwin [4] expanded on Griffith's principles to deal with fracture problems in welded steel ships that failed unexpectedly and catastrophically at cold temperatures. Under the conditions prevailing in the ship application, the material behaved in what was regarded as a brittle

fashion. Both investigators recognized that, although the analytical framework they applied was physically appropriate for linear-elastic, or brittle, behavior, the observed fracture strength was different by orders of magnitude from the values predicted by physical conditions alone.

Thus, practical applications of fracture mechanics generally require empirical correction factors to account for the actual behavior of the materials in question. During the last three decades, when fracture mechanics has developed into a recognized discipline, a frequently employed device is to force brittle behavior in a given material by making research specimens thick enough to develop essentially a plane-strain stress state at the crack tip. This device makes the linear elastic theory more nearly capable of correlating results. Unfortunately, many practical materials require that test specimens be up to 200 mm thick to produce "valid" test results. At least for aircraft structures, the practical range of thicknesses is about 1 to 35 mm. Thus, linear elastic fracture mechanics cannot deal directly with many practical problems.

To correct this deficiency, a wide variety of fracture analysis techniques have been developed. Several of these are described in other papers in the present symposium. In most cases a quasi-rigorous rationale is developed to account for some recognized phenomenon that makes real behavior different from the linear elastic behavior, and usually an empirical adjustment is ultimately required to fit the equations to actual data. The present paper follows this same pattern.

One distinguishing feature of the NASA work is best explained with the aid of Fig. 1. Ideal brittle behavior is depicted in Fig. 1(a). A center-crack tension specimen contains a crack of length c_0 and is subjected to monotonically increasing load P (plotted as the ordinate). Because all behavior is linear, the load may be increased without appreciable crack growth until a critical value P_{crit} is reached, at which time the specimen suddenly fails. As indicated earlier, this behavior is rare, even in materials regarded as brittle.

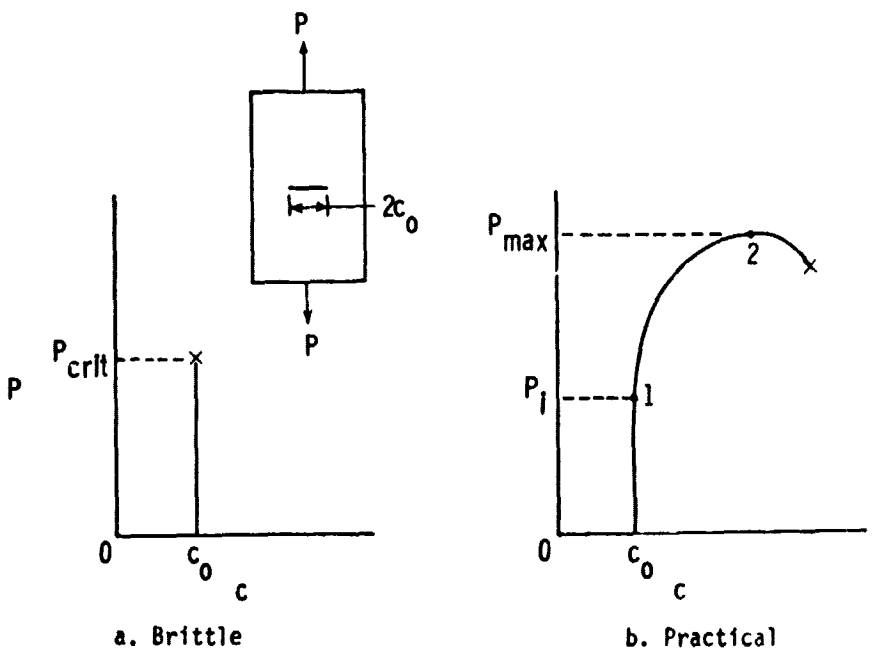

a. Brittle b. Practical

Fig. 1 Fracture of ideal and practical materials

ORIGINAL PAGE IS
OF POOR QUALITY

Practical materials behave as depicted in Fig. 1(b). A similar specimen with the same size original crack is subjected to steadily increasing load. At point 1, the crack begins to grow slowly and stably. Depending on the material and configuration, considerable crack growth and local plasticity accompany increasing load until an instability is reached at point 2. The various "improved" fracture analysis methods are directed toward answering an assortment of basically different questions. Some characterize the conditions for initiation of crack growth (point 1), others characterize the instability point (2), and do so in conjunction with identifying the corresponding crack length at the instant of instability, still others define the complete curve between 1 and 2.

The NASA work seeks to characterize the maximum load supported by the specimen just before failure and to associate that load with the initial crack length. This relationship is, of course, not located on the crack growth curve, but it answers a question of fundamental significance to designers and operators of practical hardware.

Fatigue Crack Propagation

Paris [5] was one of the first to apply fracture mechanics principles to the correlation of crack propagation data for tests under constant amplitude loading. He employed linear elastic analyses and proposed a simple power law to relate the crack growth per cycle with the range of the stress intensity caused by the load fluctuation in a given cycle for the crack configuration in question. Since that time, the simple power law has been shown to require adjustments to account for: an apparent threshold below which cracks appear not to grow; stress intensities approaching the critical intensity where unstable crack growth is expected; commonly observed effects of mean and maximum stresses; and nonlinear effects observed when a complex time history of loads is employed.

Investigations to account for these pheromena employ a wide variety of empirical or semiempirical methods with varying degrees of success. As is explained in a later section, the NASA work is based on consideration of crack closure during the load cycle, a basic phenomenon first observed and quantified by Elber [6].

Effects of Complex Configuration

All analyses of crack behavior require a basic stress analysis of the specimen or structural member under consideration. Generally, the local stress intensity is derived as a function of the shape of the part, the loading, the mode of crack deformation, dimensions of the crack (length and depth) relative to dimensions of the part (width and thickness), and plane strain or plane stress conditions at the crack front. Several catalogs of such solutions have been published [7-9] and are widely used. However, some published solutions disagree significantly or fail to account for some significant, but mathematically intractable, feature. Recent developments of high-speed computers have led to solutions for much more complicated configurations, including several in three dimensions. Although NASA work has contributed to the analysis of several unique cases [10-13], these will not be discussed in this paper. However, a later section deals with the analysis of complex structural assemblies to illustrate how such configurations can be treated.

A TWO-PARAMETER FRACTURE CRITERION

As indicated earlier, NASA work on fracture has sought to predict the maximum load that can be carried by a cracked part. Because linear elastic analyses, by themselves, were incapable of dealing with fracture in practical cases where considerable stable crack growth and plasticity occurred, a new criterion was developed [14-15]. Two parameters were involved in the final relation, which was derived from a combination of stress intensity and stress redistribution considerations. The criterion is expressed as

$$K_F = \frac{K_{Ie}}{1 - m\left(\frac{S_n}{S_u}\right)} \quad \text{when} \quad S_n < \sigma_{ys} \tag{1}$$

where

- K_{Ie} is the elastic stress intensity at failure.
- S_n is the nominal stress on the net section at failure.
- S_u is the nominal stress required to produce a plastic hinge on the complete net section, using the ultimate tensile strength of the material as the maximum stress.
- K_F is an empirically adjusted material constant having the same dimensions as an elastic stress intensity.
- m is an empirically adjusted material constant whose value must lie between zero and one.

Because two constants require adjustment, at least two (preferably considerably different) tests must be conducted to characterize the material. The parameter m is multipled by the stress ratio S_n/S_u and is thought of as representing a plasticity correction. Its value is 0 if the material is essentially brittle and 1 if the material is highly ductile. The parameter K_F is thought to be an inherent fracture strength, dependent on thickness, but independent of in-plane configuration and loading.

This criterion has been applied in the analysis of a large quantity of data taken from the published literature and from NASA tests. A partial list of parameters represented in these data follows:

Crack configurations:
- Center crack tension
- Compact
- Notch bend
- Surface cracks
- Corner cracks at holes
- Through-cracks and surface cracks in pressurized cylinders

Materials:
- Steels
- Titanium alloys
- Aluminum alloys
- Brasses
- Magnesium alloys

Thickness range: 0.5 mm to 50 mm
Width range: 25 mm to 1250 mm

ORIGINAL PAGE IS
OF POOR QUALITY

In all cases, the criterion depicted the appropriate trends among related sets of data. When two or more sets of data were available for the same material and the same thickness but systematically different specimen configurations, the criterion predicted failure loads for one set when the fracture parameters obtained for another set were used. Two representative treatments [16-17] are shown in Figs. 2 and 3.

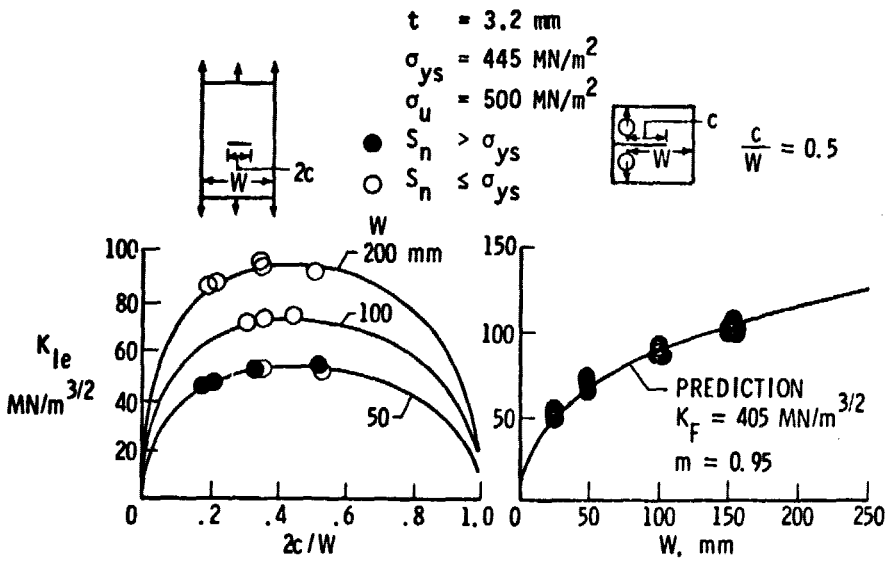

a. Curves fitted to data

b. Curves predicted from other data

Fig. 2 Correlation of fracture tests of Hiduminium H-48 alloy

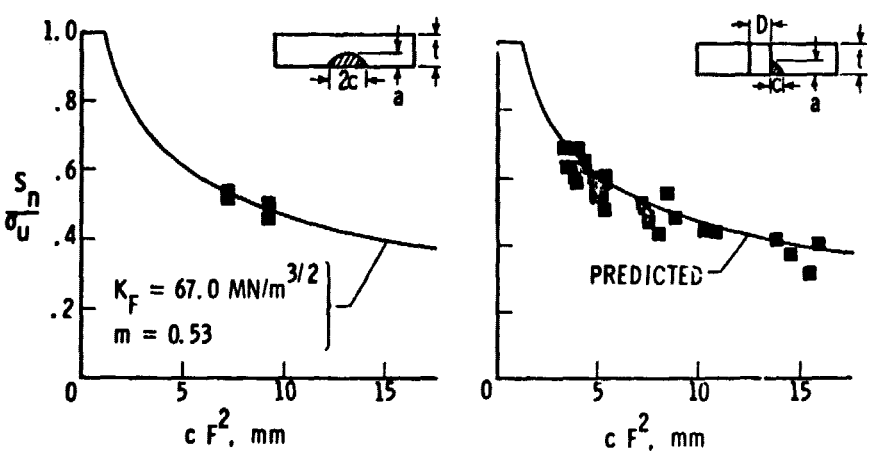

a. Curves fitted to data

(b) Curve predicted from other data

Fig. 3 Correlation of fracture tests of 2219-T87 aluminum alloy

Figure 2 is for two series of tests on a British aluminum alloy, called Hiduminum H-48 [18]. Center cracked tension specimens with several widths and various crack lengths were tested. The two parameters were determined for best fit with all the results shown in Fig. 2(a). These same values of the fracture parameters were then employed to predict the behavior of the compact specimen results shown in Fig. 2(b). In Fig. 3 the results of tests of 2219-T87 aluminum alloy specimens with surface and corner cracks [19] are treated in similar fashion. In Fig. 3(a) the two parameters were determined to achieve a best fit with test results from surface-cracked tension specimens. Figure 3(b) shows that predictions from the criterion and the parameters found in Fig. 3(a) agreed well with results of tension tests on specimens having corner cracks near holes.

Although no physical reason can be cited for establishing a correlation between the values of K_F and m, a cross-plot of these two parameters for a wide variety of materials and specimen configurations is shown in Fig. 4. The values of K_F were normalized by E, the elastic modulus for each material, to permit comparison of several classes of alloys. Although no generality of this relationship is claimed at this date, the points fall into a reasonably small scatter band. The simple relation $m = \mathrm{Tanh}\left(\frac{AK_F}{E}\right)$ has been plotted to represent this correlation.

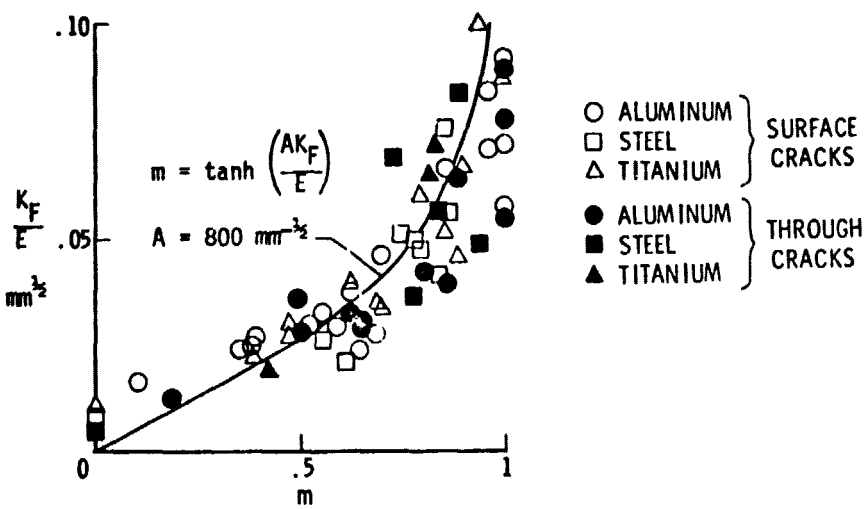

Fig. 4 Apparent relation between K_F and m

FATIGUE CRACK PROPAGATION

Constant-Amplitude Loading

As indicated earlier, the direct application of the simple power law to predict fatigue crack propagation is inadequate for several reasons. Elber [6] was the first to identify and quantify the phenomenon of crack closure. He showed persuasively that, in materials that display appreciable ductility, the crack surfaces near the crack tip may close before a specimen is completely unloaded. Such behavior is not expected in elastic specimens until at least an infinitesimal compression load is applied.

The reason for the crack closure is depicted in Fig. 5. The presence of a plastic zone ahead of a crack tip (shown with double cross hatch) is

ORIGINAL PAGE IS
OF POOR QUALITY

generally accepted as a feature of crack behavior in practical materials. The feature that had been commonly ignored was that the material adjacent to the crack surfaces near a crack tip had once been in this plastic zone, and thus, had been deformed in tension to a size larger than the original size. Consequently, as the load on a specimen is reduced, this material forces the crack surfaces to meet, to transfer compressive forces across the interface, and perhaps to produce reversed plasticity (compression) in the previously deformed material, all before the load is reduced to zero. Many investigators have conducted detailed experiments to convince themselves and others that this phenomenon exists. The intuitive consequence of this behavior is that those portions of a load cycle during which the crack tip is closed will not contribute the crack propagation.

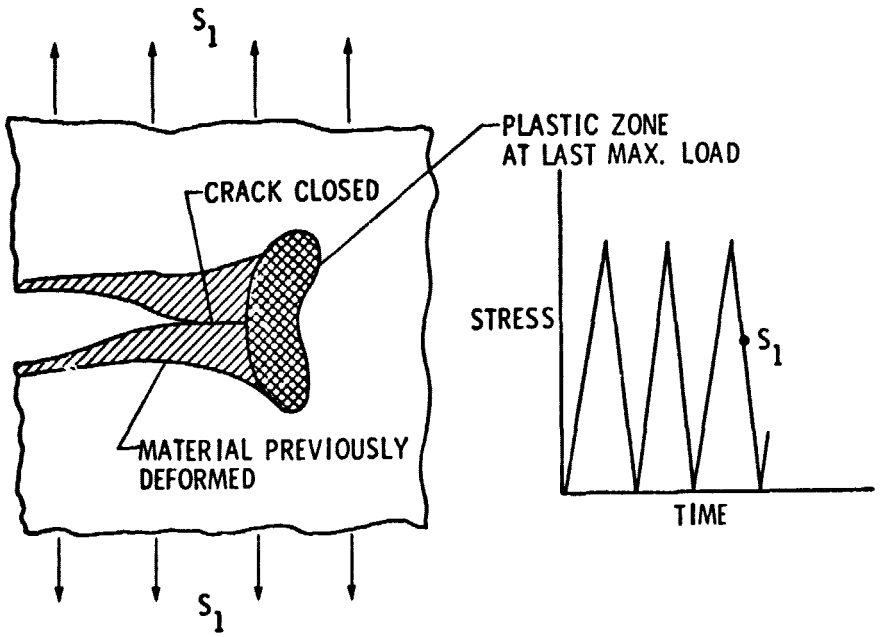

Fig. 5 Crack closure concept

In his early work, Elber [20] measured crack opening displacements near the crack tip to quantify the "crack opening stress level." He found a reasonably consistent agreement between test data on aluminum alloy specimen and the relation:

$$S_o = S_{max}\left(0.5 + 0.1R + 0.4R^2\right) \quad \text{if} \quad -0.1 \leq R \leq 0.7 \tag{2}$$

where

S_o is the stress level at which the crack tip opens
S_{max} is the maximum stress applied
R is the ratio S_{min} S_{max}

More recently, Newman [21] analyzed this behavior using a two-dimensional, elastic-plastic, finite-element analysis and showed quantitatively that cracks open and close at predictable stress levels. The finite-element analysis was shown to be quite accurate but was very complicated and required a large computing facility. More recently, Newman [22] analyzed this behavior with a simple strip-yield model that requires only a small computer and can accommodate many hundreds of thousands of variable load cycles. The region near the crack tip was modeled by bar elements having dimensions as suggested by the small rectangles in Fig. 6. An elastic-perfectly-plastic stress-strain curve was assumed. The yield stress level was adjusted to a value 15 percent greater than the actual yield stress of the material to compensate for some biaxiality that is expected in the highly stressed region. The rectangles in Fig. 6 show the extent of plastic deformations during the present and preceding load cycles. The vertical gaps between rectangles depict the crack opening. In the analysis, the amount of crack growth in a given cycle is introduced into the calculation by the analyst and is based on the effective stress range (Eq. (2)) and the simple power law for crack growth in the material. The stress distribution in the lower left of the figure shows the local stress to be zero where the crack is open, equal to the effective yield stress in the plastic zone, and the elastic values elsewhere.

Upon unloading (right side of Fig. 6), the release of elastic strains throughout the model forces the crack surfaces to approach each other, touch, transfer compression force and undergo reversed plastic deformation when appropriate. The stress distribution in the lower right shows the local stress to be zero where the crack is open, to equal the effective compressive yield stress where reversed plasticity has occurred (ω) and to have elastic values elsewhere. This model also accounts for compressive yielding at the crack surfaces, if appropriate.

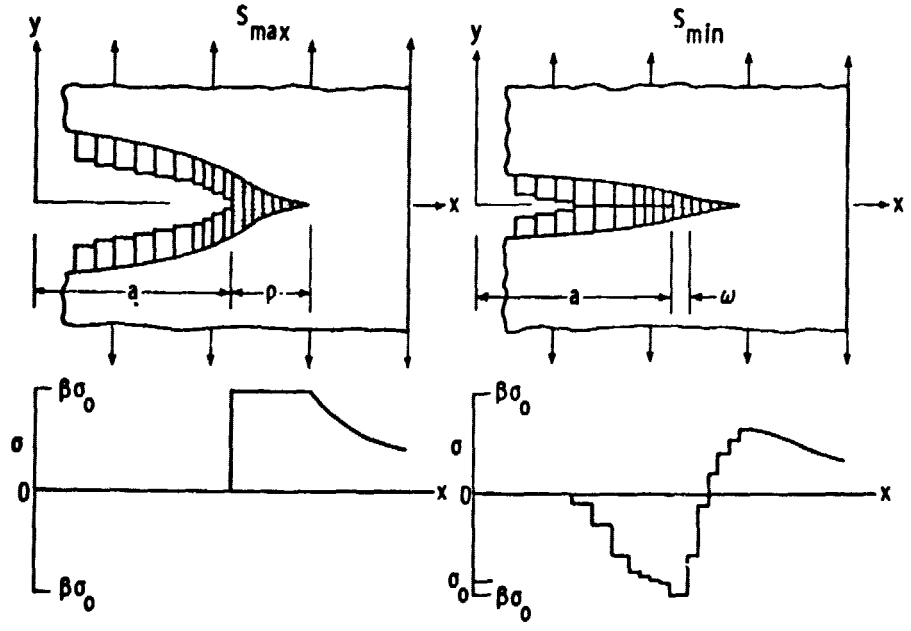

Fig. 6 Calculations of local stresses and deformations

ORIGINAL PAGE IS
OF POOR QUALITY

This model has been used to predict the crack-opening stress level for any combination of maximum and minimum stress and for prior cyclic load history. Figure 7 shows the crack-opening stresses normalized by S_{max} plotted against the ratio of S_{max} to the effective flow stress (σ_0). The effective flow stress is assumed to be the average between yield stress and ultimate tensile strength.

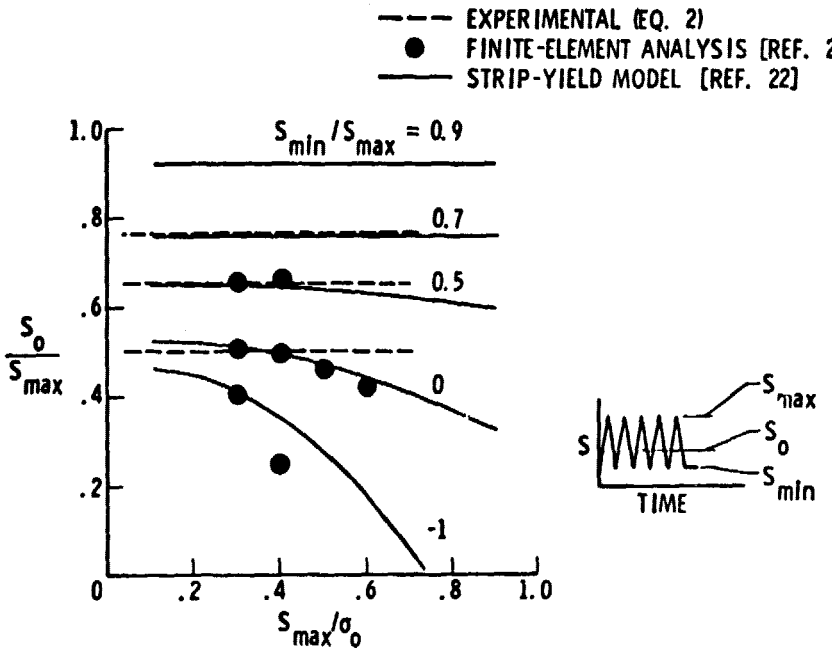

Fig. 7 Experimental and predicted crack opening stresses

The results in Fig. 7 were used to analyze fatigue crack propagation data for 7075-T6 aluminum alloy center-cracked sheet specimens [23] with a broad range of R values and maximum stresses. In Fig. 8 the basic data are shown plotted in the conventional form of growth per cycle against the range of the elastic stress intensity factor. The several discrete lines of test data reflect the R effect.

The same data are shown in Fig. 9 except that the range of stress intensity was adjusted for two effects. First, crack closure effects were accounted for by:

$$\Delta K_{eff} = (S_{max} - S_o)\sqrt{\pi a}\, F \qquad (3)$$

where

S_o is the crack opening stress level

$\sqrt{\pi a}\, F$ is the usual parameter that accounts for specimen configuration.

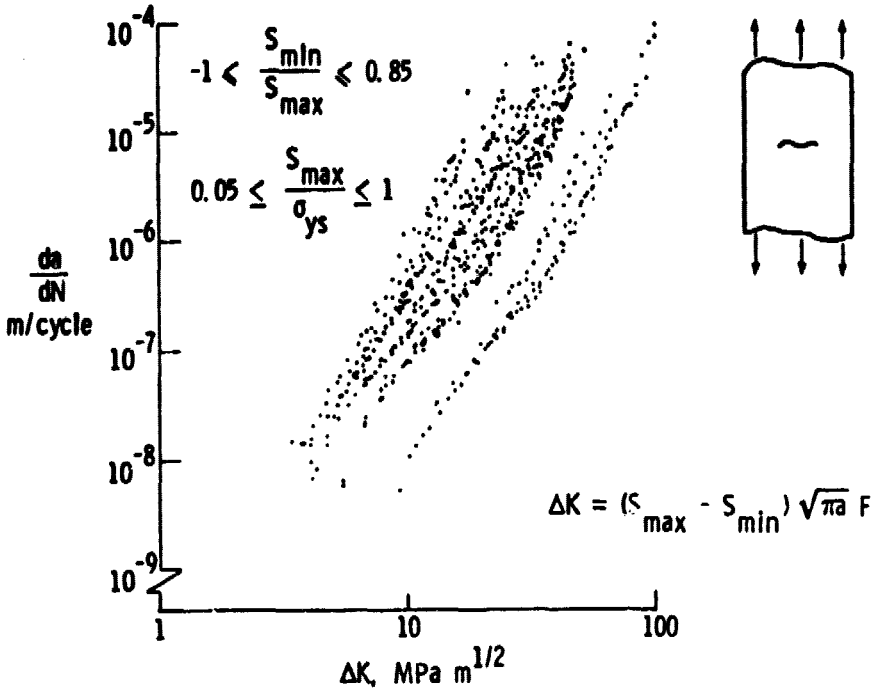

Fig. 8 Crack growth data from tests at various R values, 7075-T6 aluminum alloy sheet

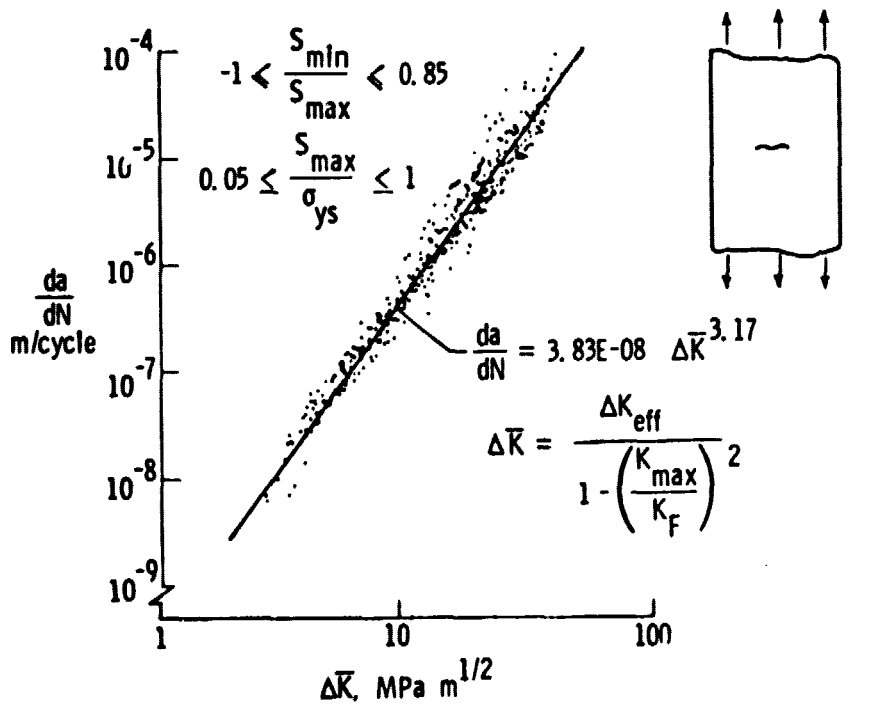

Fig. 9 Correlation of crack growth data from tests at various R values, 7075-T6 aluminum alloy sheet

ORIGINAL PAGE IS
OF POOR QUALITY

Second, the effect of high stresses was accounted for by:

$$\overline{\Delta K} = \frac{\Delta K_{eff}}{1 - \left(\frac{K_{max}}{K_F}\right)^2} \qquad (4)$$

where

K_{max} is the stress intensity corresponding to S_{max}
K_F is the fracture parameter discussed earlier.

This equation has a form similar to an empirical equation first proposed by Forman [24] to account for mean stress and high stress effects.

All the data are seen to fall in a very much narrower scatter band, indicating that the adjustments for crack closure, R effects, and maximum-stress effects are appropriate. A simple power law has been fitted to these transformed data. Obviously, this law must not be used below a threshold value, which was not established for these data.

A similar treatment of data for 2024-T3 aluminum alloy sheet specimens [23] is shown in Fig. 10 and illustrates a similarly excellent correlation. Few other sets of data exist that cover a wide enough range of stress ratios and stress levels to make a convincing argument for this analysis. However, the method has been applied to several other smaller sets of data with encouraging results.

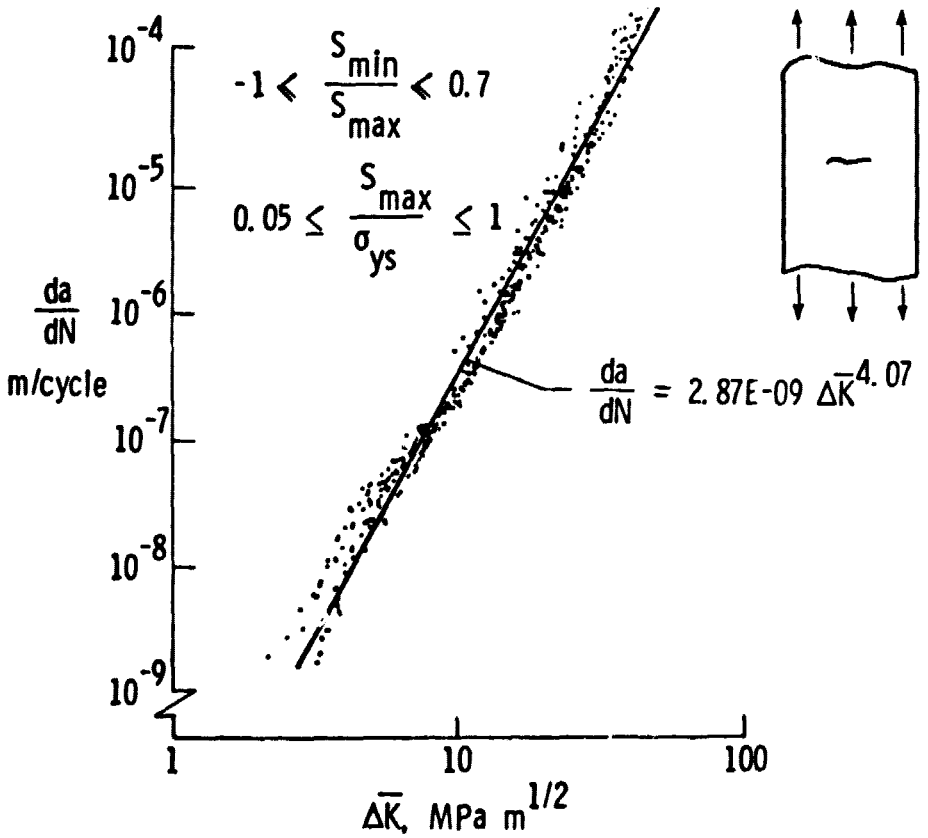

Fig. 10 Correlation of crack growth data from tests at various R values, 2024-T3 aluminum alloy sheet

Variable-Amplitude Loading

Essentially all practical crack propagation evaluations require consideration of load histories with variable amplitude loading. A strong nonlinear behavior usually called a "delay" generally follows high loads in the time history. Figure 11 illustrates a particular case. Center-cracked 2024-T3 aluminum alloy sheet specimens [22] were subjected to the simple two-amplitude loading schedule shown in the inset. The crack length is plotted against the number of load cycles. The dashed curve at the left is the behavior observed if no spike load had been applied. The symbols labeled, "Test 1" and "Test 2" represent results of two identical tests in which the spike load was applied at N = 0. These two test results are not identical because of normal scatter in behavior. However, both these tests show a "delay" of 100,000 or more cycles during which essentially no crack propagation was measured.

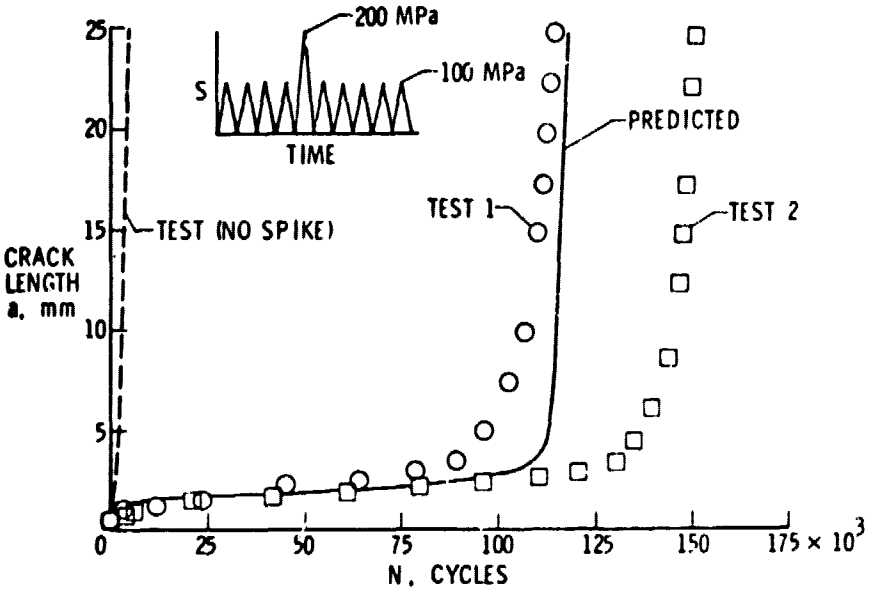

Fig. 11 Predicted and experimental crack growth in material subjected to variable amplitude loading, 2024-T3 aluminum alloy sheet

The curve labeled "Predicted" was calculated by the previously described procedure, except that the crack opening stress level associated with the spike load (computed from the simple strip-yield model) was used to define the effective range of the stress intensity. Because the crack opening stress was almost equal to the maximum stress in cycles following the spike load, essentially no crack propagation was predicted for the first 100,000 cycles of the lower stress amplitude. The prediction agrees satisfactorily with the test data.

A more complex, but practical, case of crack propagation under variable amplitude loading is shown in Fig. 12. For this example, a 2024-T3 aluminum alloy sheet specimen containing a center crack was subjected to the simulated service load history shown in the inset. For this example, the highest stress in the time history was 140 MPa. The stress on the specimen was reduced to zero periodically during each test to simulate the unloading

ORIGINAL PAGE IS
OF POOR QUALITY

of a point on the lower surface of an aircraft wing once for each flight. The number and magnitude of stresses in a given flight was varied to agree with statistical estimates of loading frequencies experienced in service of a civil transport aircraft.

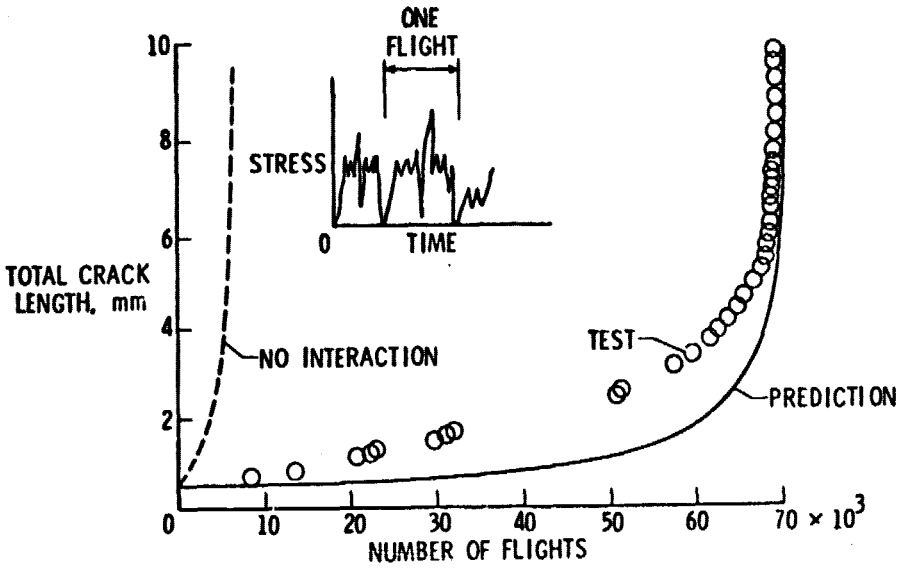

Fig. 12 Crack propagation under simulated flight loading, 2024-T3 aluminum alloy

The dashed curve on the left shows the behavior expected if crack propagation were to proceed linearly for each stress excursion (no load interaction). The test data show that the specimen survived almost 70,000 simulated flights instead of the few thousand flights expected if no load interaction were present. The predicted crack growth was again based on crack closure predicted by the strip-yield model. Although the predicted number of simulated flights was too high for crack growth between 1 and 2 mm, the predicted and experimental curves agree well for longer cracks. Further refinement of the analysis is expected to improve the agreement for short and intermediate crack lengths.

Because a given gust or maneuver load on an aircraft wing may cause a variety of local stress levels depending on detailed configurations, this analysis was repeated with the highest stress in the time history systematically varied. The predicted and experimental numbers of flights to failure are plotted as bar graphs in Fig. 13. Three values of maximum stress were assumed: 140, 170, and 200 MPa. The agreement between predictions and experimental results was excellent in each case.

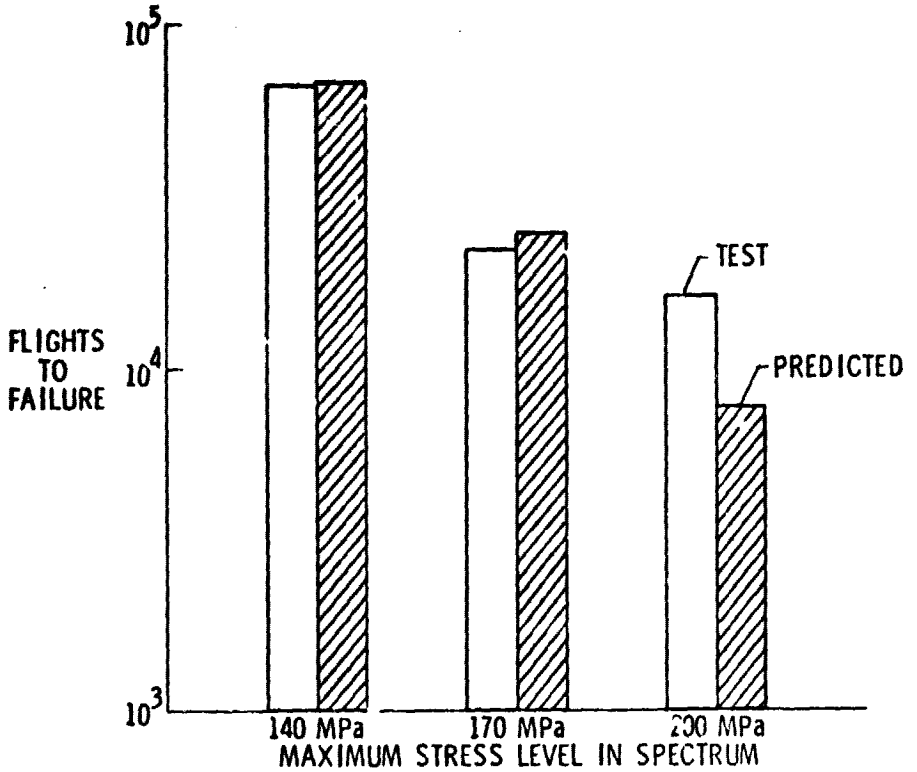

Fig. 13 Crack propagation life under simulated flight loading, 2024-T3 aluminum alloy

CRACK PROPAGATION AND FRACTURE IN BUILT-UP STRUCTURES

Aircraft wing structures are inherently composed of complex assemblies of sheets, stiffeners, splices, and doublers in order to achieve maximum strength with minimum mass and enhance damage tolerance. Thus, effective design requires that the behavior of such a structure be analyzed to determine rates of crack propagation and residual strength under service loadings.

Poe [25] has developed an analysis for calculating the stress intensity, rivet force, and stringer loads in a stiffened panel containing an initial crack. The sketch at the top of Fig. 14 depicts a typical configuration that has been analyzed. The analysis accounts appropriately for the several configuration parameters listed in the figure. The ordinate of the plot has two scales: (1) the stress intensity in the sheet normalized by the stress intensity for an unstiffened sheet containing a crack of equal length; and (2) the load in the central stringer normalized by the load in that stringer if no crack were present. The abscissa is the half-length of the crack and corresponds to the crack length shown in the sketch. According to the analysis, the stress intensity in the sheet is reduced significantly as the crack tip passes each stiffener. This illustrates that stringers can influence crack growth rates significantly. The amount by which the stress intensity is reduced depends on the specific values of each of the configurational parameters listed.

ORIGINAL PAGE IS
OF POOR QUALITY

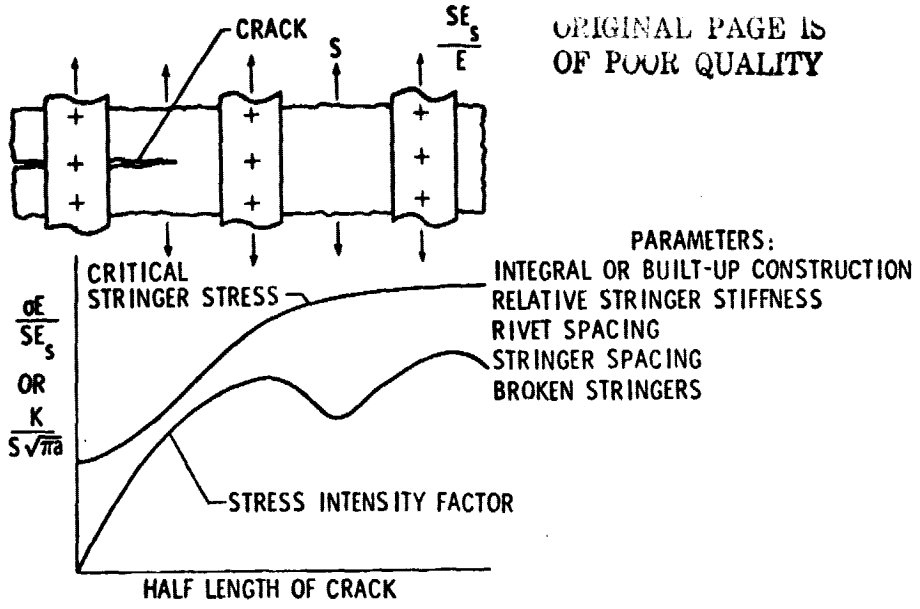

Fig. 14 Stress analysis of stiffened panels containing damage

Predictions from this analysis have been compared with rates of crack propagation observed [26] in fatigue tests conducted on systematically varied configurations and stress levels. The trends in the data were always predicted appropriately and good quantitative agreement was achieved for each case.

The upper curve in Fig. 14 illustrates that the central stringer carries a progressively higher share of the load in the structure as the crack grows. This load levels off when the crack passes other stringers, because those stringers then carry higher loads.

The residual static strength of a stiffened structure containing a crack has been assessed on the basis of this analysis. Such an assessment is described in Fig. 15. In this case, the stress required to cause static failure in the sheet or in the stringer is plotted as the ordinate. The two-parameter fracture criterion, described earlier, was used to predict the failing stress level in the 2024-T3 aluminum alloy sheet, and the ultimate tensile strength of the stringer material was used to predict the failing stress level for the stringers. Stringer 1 was assumed failed at the outset. The crack length in the sheet is plotted on the abscissa and alined with the sketch of the panel in the inset.

If the stress is progressively increased on a panel containing the crack length shown, the predicted sequence of failure events is shown by the path marked with arrows. No failure occurs until the applied stress reaches the level of point A, when the sheet is expected to fail. Because the residual strength is less than A for all crack lengths between A and B, the failure will extend to B, but will be arrested there, because more stress must be applied for crack lengths longer than B. As the stress is increased the crack will grow until point C is reached. At C, stringer 2 will have reached its ultimate tensile strength and will fail. Because the forces formerly carried by this stringer are suddenly transferred to the sheet, the load carrying capability of the sheet is suddenly reduced to the level labeled D. Thus, unless the load is removed instantaneously, the crack will quickly extend to point E where stringer S3 will fail and all

other parts of the cross section will fail in turn, because the residual strength never again exceeds the level of C.

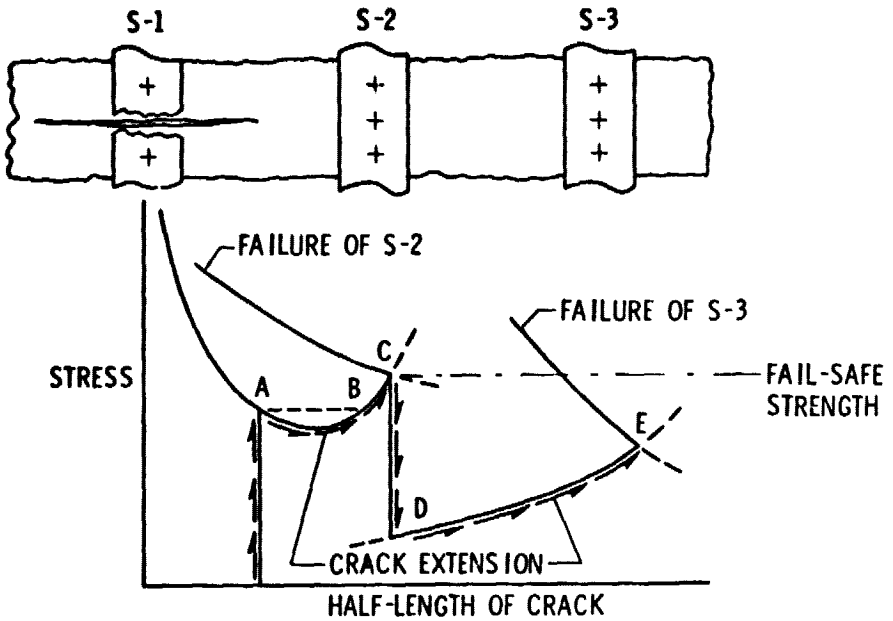

Fig. 15 Fail-safe strength prediction

The relative stiffnesses of the sheet and stringers, stringer spacings, rivet spacings, and other configurational parameters modify the relative positions of the several curves in Fig. 15. Thus, effective design requires that a range of these parameters be evaluated to produce the most damage resistant configuration with minimum weight and cost.

To facilitate this analysis, a first-generation computer program [27] has been written to deal with this design problem. The program predicts both the rate of crack propagation and the residual strength of a built-up configuration under service loadings. From these considerations the best configuration may be chosen and the allowable stress levels may be adjusted to provide the desired characteristics. Other computer programs are available to deal with other disciplinary concerns, such as original static strength, stiffness, flutter, and buckling, so that the design satisfying several criteria may be achieved with minimum weight penalty.

CONCLUDING REMARKS

This paper has reviewed systematic research that has led to improved

1. Stress intensity solutions for laboratory specimens
2. Fracture criterion for practical materials
3. Crack propagation predictions that account for mean stress and high maximum stress effects
4. Crack propagation predictions for variable-amplitude loading
5. Prediction of crack growth and residual strength in built-up structure assemblies

ORIGINAL PAGE IS
OF POOR QUALITY

These several capabilities have been incorporated into a first-generation computerized analysis that allows design for damage tolerance and trade-offs with other disciplines to produce efficient designs that meet current airworthiness requirements.

REFERENCES

1 Anon, Airplane Damage Tolerance Requirements. Military Specification MIL-A-83444 (USAF), 1974. U. S. Government Printing Office, Washington, DC.

2 Anon, Code of Federal Regulations, Title 14, Aeronautics and Space, Part 25, 1977. U. S. Government Printing Office, Washington, DC.

3 Griffith, A. A.: "The Phenomena of Rupture and Flow in Solids," Transactions, Royal Soc. London, Vol. 221, 1920.

4 Irwin, G. R., "Analysis of Stresses and Strains Near the End of a Crack Traversing a Plate," Transactions, Am. Soc. Mech. Engrs., J. of Applied Mech., 1957.

5 Paris, P. C., Gomez, M. D., and Anderson, W. E., "A Rational Analytical Theory of Fatigue," The Trend in Engineering, University of Washington, Vol. 13, No. 1, January 1961.

6 Elber, Wolf, "Fatigue Crack Closure Under Cyclic Tension," Eng. Fracture Mech. Journal, Vol. 2, pp. 37-45, 1970.

7 Tada, H., Paris, P., and Irwin, G., "The Stress Analysis of Cracks Handbook," Del Research Corporation, 1973.

8 Sih, G. C., "Handbook of Stress Intensity Solutions," Lehigh University, 1973.

9 Rooke, D. P., and Cartwright, D. J., "A Compendium of Stress Intensity Factors," Her Majesty's Stationery Office, Atlantic House, Holborn Viaduct, London, 1976.

10 Newman, J. C., Jr., "An Improved Method of Collocation for the Stress Analysis of Cracked Plates with Various Shaped Boundaries," NASA TN D-6376, August 1971.

11 Newman, J. C., Jr., "Stress Analysis of the Compact Specimen Including the Effects of Pin Loading," Fracture Analysis, ASTM STP-560, pp. 105-121, 1974.

12 Raju, I. S., and Newman, J. C., Jr., "Three-Dimensional Finite-Element Analysis of Finite-Thickness Fracture Specimens," NASA TN D-8414, May 1977.

13 Raju, I. S., and Newman, J. C., Jr., "Improved Stress-Intensity Factors for Semi-Elliptical Surface Cracks in Finite-Thickness Plates," NASA TM X-72825, August 1977.

14 Newman, J. C., Jr., "Fracture Analysis of Surface- and Through-Cracked Sheets and Plates," Engr. Fracture Mech. Journal, Vol. 5, pp. 667-689, 1973.

15 Newman, J. C., Jr., "Fracture Analysis of Various Cracked Configurations in Sheet and Plate Materials," Properties Related to Fracture Toughness, ASTM STP-605, pp. 104-123, 1976.

16 Newman, J. C., Jr., "Predicting Failure of Specimens with Either Surface Cracks or Corner Cracks at Holes," NASA TN D-8244, June 1976.

17 Newman, J. C., Jr., "Fracture Analysis of Surface- and Through-Cracks in Cylindrical Pressure Vessels," NASA TN D-8325, December 1976.

18 Adams, N. J. I., and Murro, H. G., "A Single Test Method for Evaluation of the J-Integral as a Fracture Parameter," Engr. Fracture Mech. Journal, Vol. 16, No. 1, 1974.

19 Masters, J. N., Bixler, W. D., and Finger, R. W., "Fracture Characteristics of Structural Aerospace Alloys Containing Deep Surface Flaws," NASA CR-134587, 1973.

20 Elber, Wolf, "The Significance of Fatigue Crack Closure," Damage Tolerance in Aircraft Structures, ASTM STP-486, pp. 230-242, 1971.

21 Newman, J. C., Jr., "A Finite-Element Analysis of Fatigue Crack Closure," Mechanics of Crack Growth, ASTM STP-590, pp. 281-301, 1976.

22 Newman, J. C., Jr., "Correlation of Fatigue-Crack-Growth Rates Using a Simple Crack-Closure Model," presented at the 1977 SESA Spring Meeting, Dallas, TX, May 15-20, 1977.

23 Hudson, C. M., "Effect of Stress Ratio on Fatigue-Crack Growth in 7075-T6 and 2024-T3 Aluminum-Alloy Specimens," NASA TN D-5253, 1969.

24 Forman, R. G., Kearny, V. E., and Engle, R. M., "Numerical Analysis of Crack Propagation in Cyclic-Loaded Structures," J. of Basic Eng., Trans. of ASME, Series D, Vol. 89, No. 3, pp. 459-464, September 1976.

25 Poe, C. C., Jr., "Stress Intensity Factor for a Cracked Sheet with Riveted and Uniformly Spaced Stringers," NASA TR R-358, May 1974.

26 Poe, C. C., Jr., "Fatigue Crack Propagation in Stiffened Panels," Damage Tolerance in Aircraft Structures, ASTM STP-486, pp. 79-97, 1971.

27 Kruse, G. S., "An Automated Procedure for Preliminary Design of Primary Structure for Transport Aircraft," ASME Preprint 76-WA/Aero 9, December 1976.

1. Report No.	2. Government Accession No.	3. Recipient's Catalog No.
NASA TM 78766		

4. Title and Subtitle	5. Report Date
RECENT DEVELOPMENTS IN ANALYSIS OF CRACK PROPAGATION AND FRACTURE OF PRACTICAL MATERIALS	JUNE 1978
	6. Performing Organization Code: 2530

7. Author(s)	8. Performing Organization Report No.
H. F. HARDRATH, J. C. NEWMAN, JR., W. ELBER, C. C. POE, JR.	
	10. Work Unit No.: 505-02-33-03
9. Performing Organization Name and Address: NASA LANGLEY RESEARCH CENTER, HAMPTON, VA 23665	11. Contract or Grant No.
	13. Type of Report and Period Covered: TECHNICAL MEMORANDUM
12. Sponsoring Agency Name and Address: NATIONAL AERONAUTICS AND SPACE ADMINISTRATION, WASHINGTON, DC 20546	14. Sponsoring Agency Code

15. Supplementary Notes

PAPER TO BE PRESENTED AT THE INTERNATIONAL SYMPOSIUM OF FRACTURE MECHANICS, SEPTEMBER 11-13, 1978, WASHINGTON, DC.

16. Abstract

Current U.S. Air Force and proposed U.S. civil airworthiness regulations are based on two evaluations. First, the rate of damage propagation under expected service loading; and second, the residual static strength in the presence of significant damage. Both of these evaluations employ fracture mechanics analyses.

Unfortunately, most fracture mechanics developments have concentrated on analysis and prediction of behavior in brittle materials and relatively simple heavy sections for which simple linear elastic analysis are adequate. In contrast, aircraft structures usually employ somewhat ductile materials, thin gages, and complex configurations. Further, complex load histories and hostile environments are generally features of most aircraft design problems. Consequently, special considerations are required to treat these problems adequately.

NASA Langley Research Center has conducted a variety of research tasks to extend the capabilities of fracture mechanics to deal with some of these complexities. The purpose of this paper is to describe the current stage of development of these capabilities.

17. Key Words (Suggested by Author(s))	18. Distribution Statement
CRACK PROPAGATION FRACTURE METALLIC MATERIALS STRESS-INTENSITY FACTOR STRUCTURES	UNCLASSIFIED - UNLIMITED

19. Security Classif. (of this report)	20. Security Classif. (of this page)	21. No. of Pages	22. Price*
UNCLASSIFIED	UNCLASSIFIED	18	$4.00

* For sale by the National Technical Information Service, Springfield, Virginia 22161